JOC The Journal of Organic Chemistry

Article

pubs.acs.org/joc

Mechanisms and Origins of Switchable Regioselectivity of Palladium- and Nickel-Catalyzed Allene Hydrosilylation with N-Heterocyclic Carbene Ligands: A Theoretical Study

Hujun Xie,*[,†] Lijiang Zhao,[†] Liu Yang,[†] Qunfang Lei,[‡] Wenjun Fang,[‡] and Chunhua Xiong*[,†]

[†]Department of Applied Chemistry, School of Food Science and Biotechnology, Zhejiang Gongshang University, Hangzhou 310035, People's Republic of China

[‡]Department of Chemistry, Zhejiang University, Hangzhou 310027, People's Republic of China

Supporting Information

ABSTRACT: The mechanisms and origins for the Pd- and Ni-catalyzed regioselective hydrosilylation of allene have been investigated by means of density functional theory (DFT) calculations. The free-energy profiles of Pd- and Ni-catalyzed reactions with small and bulky N-heterocyclic carbene (NHC) ligands are calculated to determine the mechanism for regioselectivities. The calculation results show that different metals (Ni vs Pd) lead to regiochemical reversals for the hydrosilylation of allene. The allylsilane is the major product via palladium catalysis with small NHC ligand, while the vinylsilane is the major product via nickel catalysis with bulky NHC ligand. Both electronic and steric factors play a key role in the regioselectivities for the hydrosilylation of allene via Pd and Ni catalysts. The calculation results are in good agreement with observed regioselectivities and could provide insights into the design of new catalysts for the regioselectivity of hydrosilylation reactions.

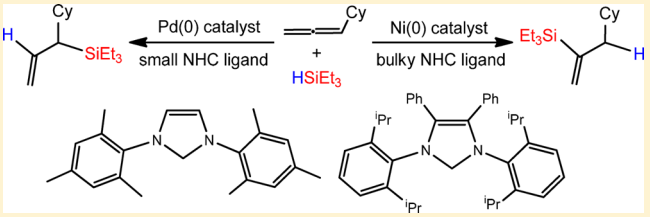

INTRODUCTION

In the past years, organosilicon compounds have appeared, acting as structural units in organic synthesis, which have been widely employed to form the C−C bond in many synthetic transformations,[1] such as Hiyama cross-coupling,[2] Sakurai-type allylation, and crotylation reactions.[3] The hydrosilylation of π-systems catalyzed by a transition metal is an important method to synthesize the organosilicon compounds.[4] For example, the hydrosilylation of alkynes can form alkenylsilanes (eq 1), and the

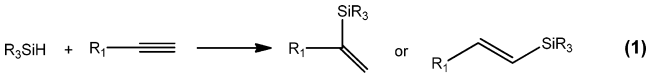

(1)

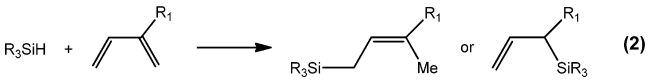

(2)

hydrosilylation of 1,3-dienes can form allylsilanes (eq 2). In these reactions, it often leads to regio- or stereoisomeric mixtures, which are very difficult to separate from each other. Thus, building a new method capable of obtaining one isomer with wide substrate scope is still a challenge.

Enormous efforts have been made for the addition of silicon hydride compounds to multiple bonds, which seems very efficient to yield the organosilicon compounds.[5] In 1947, Sommer and co-workers reported the first hydrosilylation for the reaction of trichlorosilane with 1-octene. The low selectivity was observed via a free-radical mechanism.[6] In 1953, Wagner et al. investigated the hydrosilylation of acetylene and allyl chloride via trichlorosilane catalyzed by platinum supported on powdered charcoal.[7] Patroniak et al.[8] reported the synthesis of new complex of Pt(IV) with dimethylquaterpyridine ligand, which is an effective and highly selective catalyst precursor in the hydrosilylation of styrene and terminal alkynes. Hosoya et al.[9] studied the Pd-catalyzed regio- and stereoselective hydrosilylation of electron-deficient alkynes, and this method can be further used to the formation of α-silylalkenes. Moberg et al.[10] reported Pd-catalyzed addition of dimethylchlorosilane (Me_2SiHCl) to 1,3-enynes. The reaction gives dienylsilanes via addition of the silicon to the internal alkyne carbon atom. Liu et al.[11] investigated the hydrosilylation reaction of ethylene gas with trimethoxysilane catalyzed either by ruthenium trichloride hydrate alone or by ruthenium trichloride hydrate doped with iodine. The results indicated that the hydrosilylation reaction of ethylene gas with trimethoxysilane was a first-order reaction process.

The relevance of the selectivity of catalyzed hydrosilylation has been extensively developed for synthetic applications to yield the desired product.[12] The hydrosilylation of alkynes could form three regioisomers: α and β-(E) and β-(Z) (eq 3).

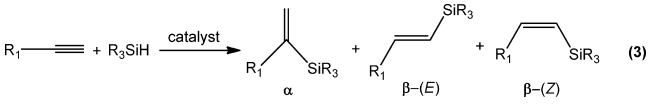

(3)

The ratio of isomers is related to the metals, ligands, alkynes, and silanes employed. The selectivity of hydrosilylation has

Received: March 8, 2014
Published: April 29, 2014

dx.doi.org/10.1021/jo500557w | J. Org. Chem. 2014, 79, 4517−4527

attracted wide interest, while only a few systems could result in one regioisomer.[13] Trost et al.[14] reported the alkyne hydrosilylation catalyzed by ruthenium complexes, and Markovnikov product was produced with high regioselectivity. This reaction could tolerate the internal alkynes to generate one olefin geometry via trans addition. Ritter et al.[15] investigated the synthesis of a well-defined Fe catalyst (bis(iminopyridine) Fe pyridine complex) and application to the regio- and stereoselective hydrosilylation of 1,3-dienes, and the product allylsilanes are formed with high selectivities.

Important developments have been made for the hydrosilylations of alkynes and alkenes, while the studies on the allene hydrosilylations have rarely been done. Yamamoto et al.[16] investigated the Lewis acid catalyzed allene hydrosilylations. The reaction can proceed via a highly regio- and stereocontrolled manner. The hydrosilylation of aromatic allenes are catalyzed by $AlCl_3$ to produce the alkenylsilanes with high regio- and stereoselectivities. Recently, Montgomery et al.[17] developed regioselective, catalyst-controlled methods for the hydrosilylation of allenes. It was found that the regioselectivity is mediated via the choice of metals. Alkenylsilanes are given by nickel catalyst with bulky N-heterocyclic carbene (NHC) ligand, while allylsilanes are formed by palladium catalyst with small NHC ligand.

Despite important contributions from experimental results, the detailed reaction mechanisms for regioselectivity of allene hydrosilylation are still elusive because no intermediates are isolated for the present catalytic reactions; thus, the experiments cannot explain why different transition metals and ligands can give the different products. In this paper, the reaction mechanisms for the Pd- and Ni-catalyzed hydrosilylation of allenes have been studied via density functional theory (DFT), and the regioselectivities have also been explored and addressed.

COMPUTATIONAL DETAILS

All species involving in the reactions were optimized via DFT calculations at the hybrid Becke3LYP (B3LYP) level.[18] This method is reasonable and has been validated in our early work[19] and other computations on Pd- and Ni-catalyzed reaction.[20] The 6-31g(d) basis set was selected to describe the C, N, and H atoms, while the effective core potentials (ECPs) of Hay and Wadt with a double-ζ valence basis set (LanL2DZ)[21] were employed for the Pd, Ni, and Si atoms. Moreover, the polarization functions for Pd(ζ_f) = 1.472,[22] Ni(ζ_f) = 3.130, and Si(ζ_d) = 0.262 were added.[23] Frequency calculations have also been computed to confirm the stationary points as minima or transition states. To validate the transition states indeed connecting two relevant minima, intrinsic reaction coordinate (IRC) calculations were also performed.[24] The Gaussian09 software package was used for all calculations.[25]

To take the solvent effects into account, conductor-like polarizable continuum model (CPCM)[26] was used for single-point calculations based on the optimized geometries in the gas phase with the UAHF radii. In these calculations, tetrahydrofuran (THF) was selected as the solvent, corresponding to the experimental conditions.

The relative free energies and relative electronic energies maybe different owing to the entropic contributions because the numbers of reactant and product molecules are different. The gas-phase calculations can overestimate the entropic contribution; therefore, corrections were added to the free energies according to the free volume theory.[27] In the case of 1:1 or 2:2 changes, it is not necessary to add the corrections. However, in the case of two-to-one (or one-to-two) transformations, a correction of −2.6 (or 2.6) kcal/mol was made at the temperature of 298.15 K. These corrections have been confirmed by early calculation studies.[28] In these calculations, the relative free energies in the solvent were adopted to describe the reaction mechanisms.

RESULTS AND DISCUSSION

According to previous experiments,[17] the hydrosilylation of allene was described in eq 4. Two isomers are shown via the

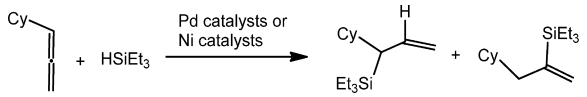

(4)

positions of the silyl group and hydrogen atom inserted into the allene. The regioselective allene hydrosilylation is governed primarily by the choice of metals, which are involved in the N-heterocyclic carbene complexes of palladium and nickel. Allylsilane is the major product via palladium catalysis with small N-heterocyclic carbene (NHC) ligand, and vinylsilane is the major product via nickel catalysis with bulky NHC ligand. Herein, we perform DFT calculations to explore the mechanisms and regioselectivities in detail.

Allene Hydrosilylation via Palladium Catalysts with N-Heterocyclic Carbene Ligands. On the basis of experimental results, Montgomery and co-workers proposed a reaction mechanism (Scheme 1),[17] including oxidative addition,

Scheme 1. Proposed Catalytic Cycle for the Allene Hydrosilylation Catalyzed by Small N-Heterocyclic Carbene Complex of Palladium for the Formation of Allylsilane

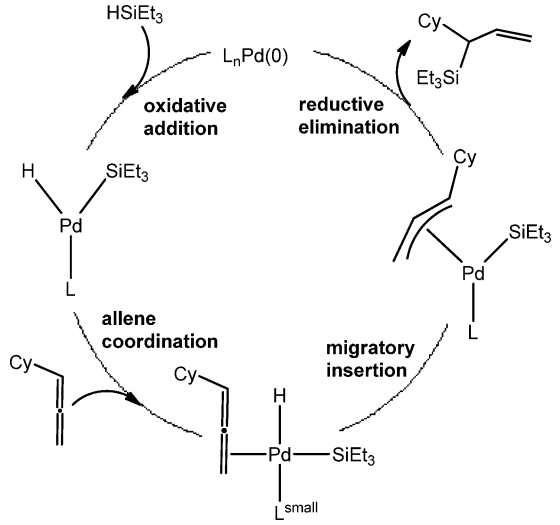

allene coordination, migratory insertion, and reductive elimination, to account for the Pd-catalyzed allene hydrosilylation for the formation of allylsilane. In the present calculations, we first consider the allene hydrosilylation catalyzed by the small N-heterocyclic carbene complex of palladium for the formation of allylsilane. The free-energy profiles for this reaction are shown in Figure 1 (path **ai**). Important structures are displayed in Figure 2.

As shown in Scheme 1, the reaction starts with the oxidative addition of Si−H bond of $HSiEt_3$ to the Pd(0) catalyst **1a**. From catalyst **1a**, $HSiEt_3$ is initially coordinated to the Pd(0) catalyst to give η^2-silane complex **2a**, and the step is exogonic by 1.3 kcal/mol (Figure 1). The transition-metal η^2-silane complexes have gained immense research interest as important intermediates in metal-catalyzed hydrosilylation reactions.[29] The Si−H bond distance in complex **2a** is calculated to be 1.620 Å (Figure 2), longer than a normal single bond according to the covalent radius predictions (Si−H =1.48 Å).[30] In contrast

dx.doi.org/10.1021/jo500557w | J. Org. Chem. 2014, 79, 4517−4527

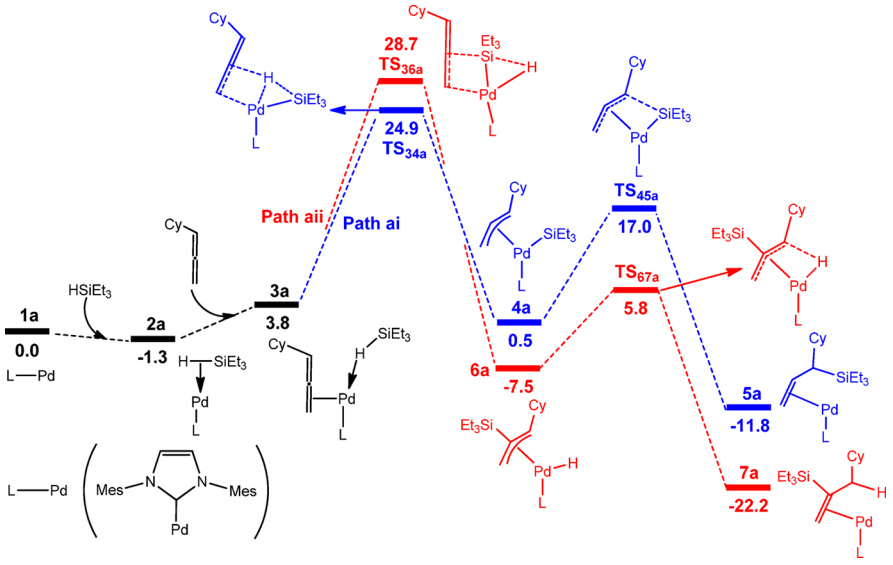

Figure 1. Free-energy profiles calculated for the allene hydrosilylation catalyzed by a small N-heterocyclic carbene complex of palladium for the formation of allylsilane (path **ai**) and vinylsilane (path **aii**). The relative free energies in the solvent are given in kcal/mol.

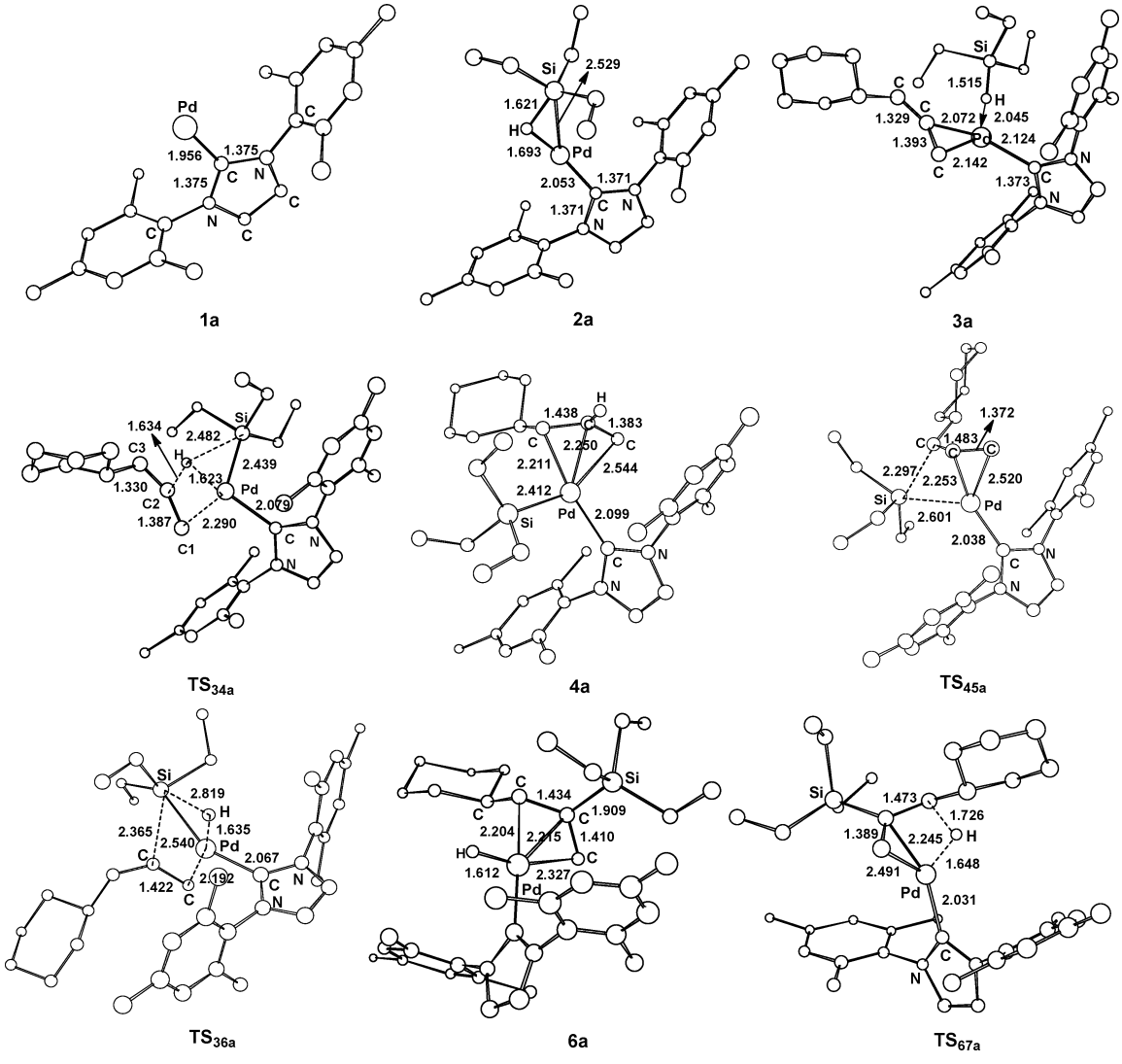

Figure 2. Optimized species involved in the allene hydrosilylation catalyzed by a small N-heterocyclic carbene complex of palladium for the formation of allylsilane and vinylsilane shown in Figure 1

dx.doi.org/10.1021/jo500557w | J. Org. Chem. 2014, 79, 4517−4527

to the normal bond length of Pd−H bond (1.56 Å), the Pd−H bond in complex **2a** is slightly lengthened with a value of 1.693 Å.[31] The Si−Pd−H bond angle in **2a** is small with a value of 39.2°. According to the calculations, the product of Si−H oxidative addition is not stable owing to the high trans effect of the hydrido ligand trans to the NHC ligand. Hence, no stationary point on the potential energy surface can be found for such a structure, which has been validated by previous calculations.[32] From **2a**, the cyclohexylallene is coordinated to the palladium center via the C═C double bond not attached to cyclohexyl(Cy) group to give an agostic complex **3a**, and this step is endergonic by 5.1 kcal/mol. Subsequent Si−H bond oxidative addition concerted with migratory insertion of hydride to allene takes place via addition to the central allene carbon to produce η^3 π-allyl complex **4a**. The similar insertion mechanism has been proposed for the hydrosilylation of terminal alkynes[33] and allene silaboration.[34] An overall barrier is calculated to be 26.2 kcal/mol from **2a** to $\mathbf{TS_{34a}}$. The hydride in $\mathbf{TS_{34a}}$ is trans to the small ligand, and the C−H and Si−H distances in $\mathbf{TS_{34a}}$ are equal to 1.633 and 2.481 Å, respectively. Accordingly, the shorter C−H and longer Si−H distances indicate that $\mathbf{TS_{34a}}$ is a later transition state. Previous studies showed that π-allyl complexes are critical intermediates in transition-metal catalyzed reactions, which can occur via reductive elimination.[35] It has been shown that the N-heterocyclic carbene ligand is symmetrical; thus, there is only one possibility for the migratory insertion step. The following C−Si reductive elimination occurs via the transition state $\mathbf{TS_{45a}}$ to generate complex **5a**. This step requires overcoming a barrier of 16.5 kcal/mol. Finally, allylsilane is produced and the palladium catalyst is regenerated.

Based on the calculation results discussed above, a revised version of the reaction cycle is given in Scheme 2. The mechanism includes three major parts: (1) coordination of $HSiEt_3$ and allene to the Pd center to afford complex **3a**; (2) subsequent Si−H bond oxidative addition concerted with migratory insertion to give the intermediate **4a**; and finally, (3) C−Si reductive elimination to produce the allylsilane product and regenerate the catalyst. The concerted step is rate-limiting and requires an overall free energy barrier of 26.2 kcal/mol from **2a** to $\mathbf{TS_{34a}}$ (Figure 1).

Scheme 2. Revised Catalytic Cycle for the Hydrosilylation of Allene via Palladium Catalyst with Small N-Heterocyclic Carbene Ligand for the Formation of Allylsilane

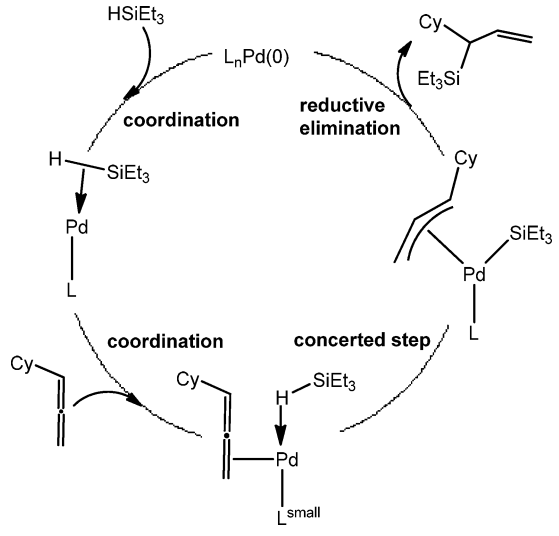

We also study the allene hydrosilylation catalyzed by the small N-heterocyclic carbene complex of palladium for the formation of vinylsilane. The reaction mechanism is shown in Scheme 3. The energy profiles in this reaction are described in Figure 1 (path **aii**). The optimized geometries are depicted in Figure 2.

Scheme 3. Proposed Catalytic Cycle for the Allene Hydrosilylation Catalyzed by a Small N-Heterocyclic Carbene Complex of Palladium for the Formation of Vinylsilane

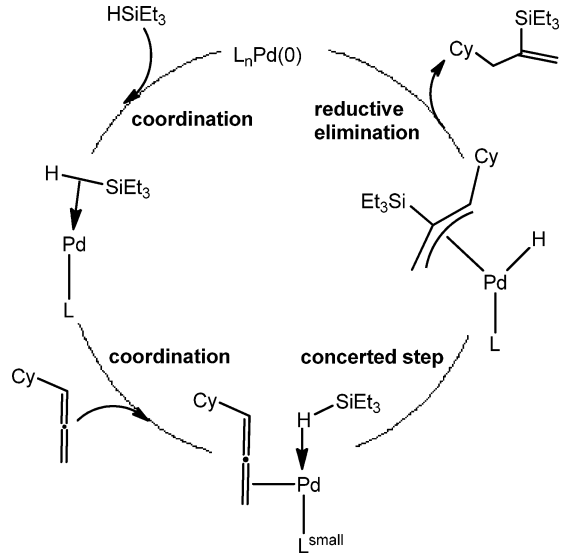

Compared to Schemes 2 and 3, we can clearly see that the differences between the two pathways are involved in the concerted and reductive elimination steps. As shown in Figure 1, the concerted step in path **ai** is related to the hydride insertion, and the reductive elimination is involved in the C−Si bond coupling, while the concerted step in path **aii** is involved in the silyl insertion and the reductive elimination is related to the C−H bond coupling. According to the calculations, the concerted step is the rate-limiting step for Pd-catalyzed allene hydrosilylation for the formation of allylsilane and vinylsilane. An overall rate-determining free energy barrier in path **aii** was calculated to be 30.0 kcal/mol from **2a** to $\mathbf{TS_{36a}}$, significantly higher than the barrier in path **ai** (26.2 kcal/mol from **2a** to $\mathbf{TS_{34a}}$) by 3.8 kcal/mol. The calculation results agree with the experimentally observed regioselectivity (allylsilane/vinylsilane = 98:2).[17]

As shown in Figure 1, allylsilane complex **5a** and vinylsilane complex **7a** are obtained, which can result in the products by Pd−L (L = ligand) decoordination. The major product **5a** is less stable by 10.4 kcal/mol than the minor product **7a**. Thus, we can conclude that the formation of allylsilane (path **ai**) is kinetically more favorable than the formation of vinylsilane catalyzed by a small N-heterocyclic carbene complex of palladium. In the rate-determining hydride insertion step for the formation of allylsilane, a hydride connects to the electron-deficient allene carbon atom to give the C−H bond, which is confirmed by the NBO charge analysis.[36] In contrast to the two terminal carbons shown in Scheme 4, the central carbon of the allene is electron-deficient. Therefore, a nucleophile (hydride)

dx.doi.org/10.1021/jo500557w | J. Org. Chem. 2014, 79, 4517−4527

Scheme 4. NBO Charges of Free Allene and TS_{34a}

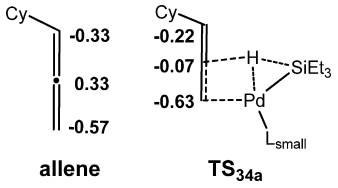

can attack the central carbon of allene.[37] In addition, the hydride insertion in TS_{34a} occurs nearly in the PdC1C2 plane (Figure 2). However, the silyl group is out-of-plane by 60° in TS_{36a}. Overall, hydride insertion is much favored over silyl insertion. These calculations are consistent with previous research by Brookhart et al.[38] that showed alkene insertion is common for M−H (M = metal) but much less common for M−Si.

The allene hydrosilylations catalyzed by the bulky N-heterocyclic carbene complex of palladium for the formation of allylsilane and vinylsilane are also explored. The free-energy profiles for the formation of allylsilane (path **bi**) and vinylsilane (path **bii**) are shown in Figure 3, and important structures are displayed in Figure 4. As depicted in Figure 3, the oxidative addition of Si−H bond concerted with hydride insertion is the rate-limiting step in path **bi** requiring a barrier (TS_{23b}) of 41.6 kcal/mol, while the Si−H bond oxidative addition concerted with the silyl insertion is the rate-determining step in path **bii** needing a barrier (TS_{25b}) of 40.2 kcal/mol. On the basis of the calculations, the barriers for both reactions are significantly high and are kinetically unfavorable under experimental reaction conditions (room temperature), which are ascribed to the strong steric interactions between the bulky NHC ligand with the silyl group and allene in TS_{23b} and TS_{25b} (Figure 4). The calculations are consistent with previous experiments that found the product yields of allylsilane and vinylsilane are very low and the regioselectivity is not determined.[17]

Allene Hydrosilylation via Nickel Catalysts with N-Heterocyclic Carbene Ligands. We first investigated the allene hydrosilylation catalyzed by the bulky N-heterocyclic carbene complex of nickel. Figure 5 shows the free energy profiles for the formation of allylsilane (path **ci**) and vinylsilane (path **cii**). The corresponding optimized structures with selected structural parameters are presented in Figure 6. The calculation results demonstrate that the catalytic mechanisms of both reactions are similar to that of Pd-catalyzed allene hydrosilylation with a bulky NHC ligand (Figure 3). Path **cii** involves the reaction for the formation of vinylsilane (Figure 5), and the Si−H bond oxidative addition concerted with silyl insertion is the rate-determining step with a barrier (TS_{23c}) of 19.2 kcal/mol. Path **ci** considers the reaction for the formation of allylsilane, and the Si−H bond oxidative addition concerted with hydride insertion is the rate-determining step with a barrier (TS_{25c}) of 23.5 kcal/mol. The barrier for path **ci** is higher by 4.3 kcal/mol than that of path **cii** (23.5 kcal/mol versus 19.2 kcal/mol), consistent with the experimentally observed regioselectivity (vinylsilane/allylsilane = 98:2).[17] The calculations also show that path **cii** is both kinetically and thermodynamically more favored than path **ci**. The relatively high barrier of TS_{25c} is ascribed to the steric repulsions between the bulky NHC ligand with the silyl group and allene (Figure 6).

In path **cii**, the reaction is started by the $HSiEt_3$ coordination to the Ni center to form η^2-complex **2c**, and the process is slightly exogonic by 2.2 kcal/mol (Figure 5). Subsequent the Si−H bond oxidative addition concerted with silyl insertion occurs to give η^3-intermediate **3c**. A barrier (TS_{23c}) of 19.2 kcal/mol is required, and the C−Si and Si−H distances in TS_{23c} amount to 2.267 and 2.354 Å, respectively (Figure 6). Finally, C−H reductive elimination step yields the intermediate **4c**, which can liberate the product vinylsilane and regenerates the catalyst. The barrier for reductive elimination (TS_{34c}) is predicted to be only 5.1 kcal/mol.

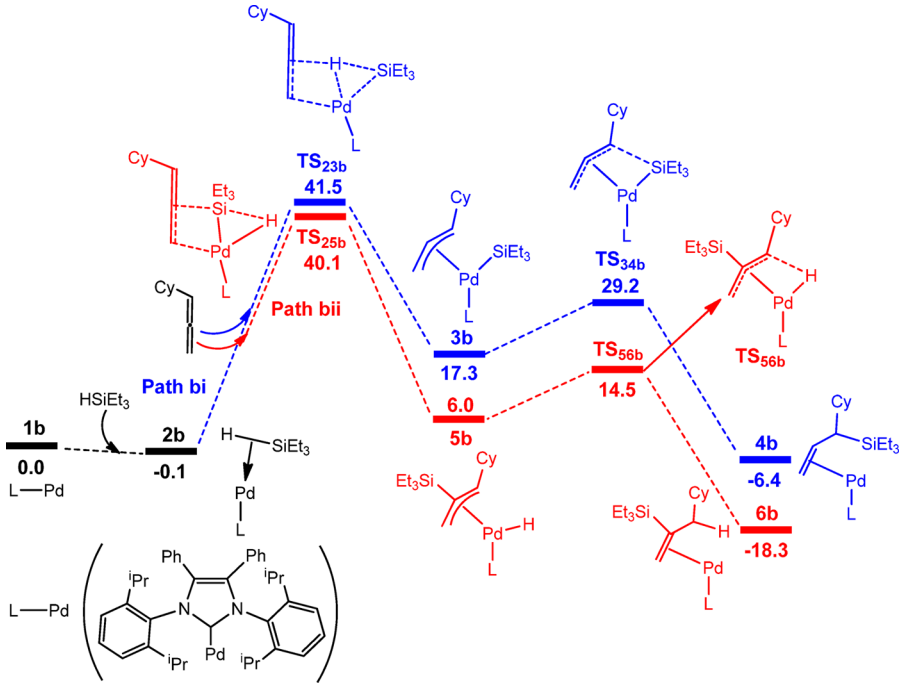

Figure 3. Free-energy profiles calculated for the allene hydrosilylation catalyzed by bulky N-heterocyclic carbene complex of palladium for the formation of allylsilane (path **bi**) and vinylsilane (path **bii**). The relative free energies in the solvent are given in kcal/mol.

dx.doi.org/10.1021/jo500557w | J. Org. Chem. 2014, 79, 4517−4527

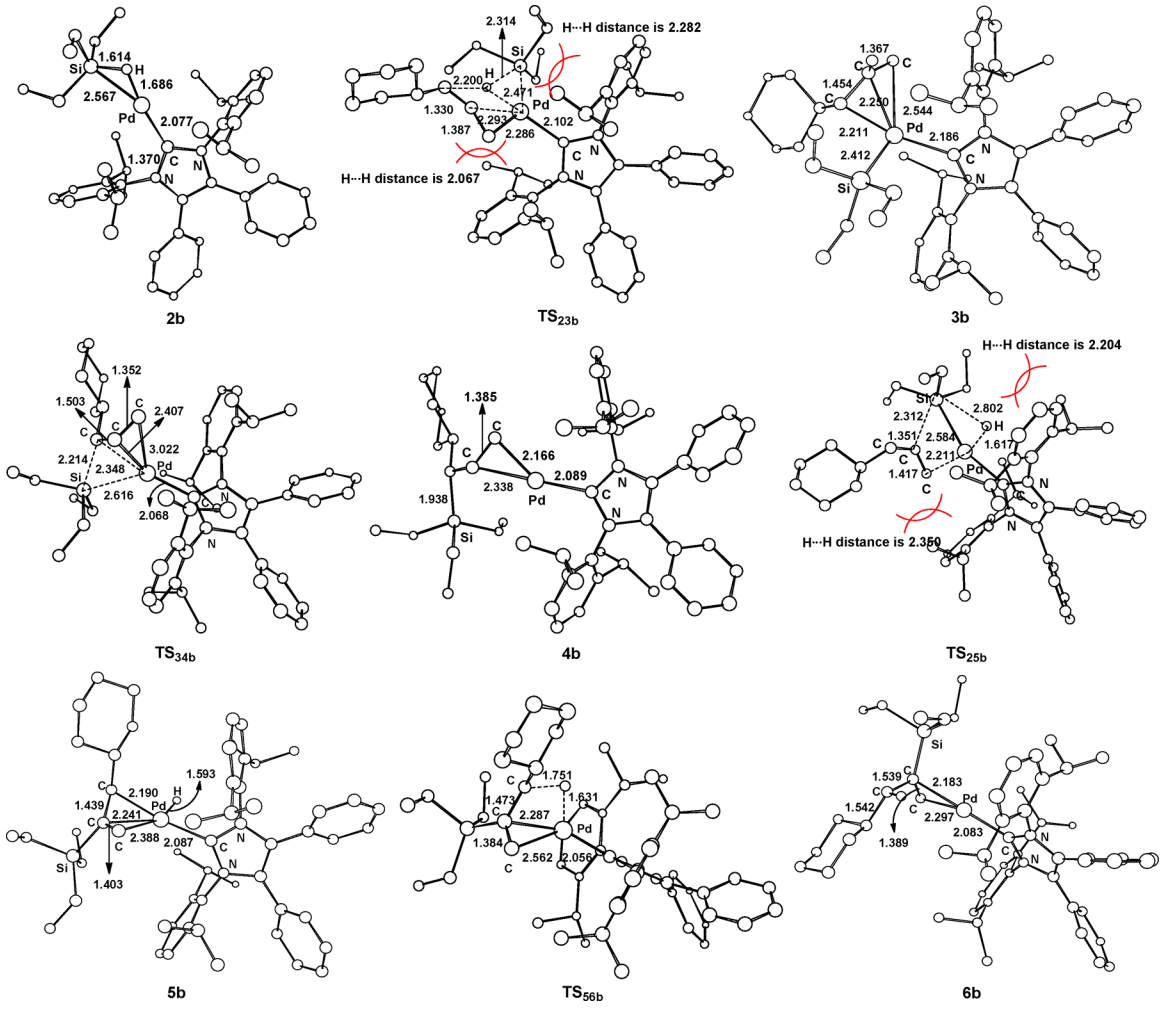

Figure 4. Optimized species involved in the allene hydrosilylation catalyzed by bulky the N-heterocyclic carbene complex of palladium for the formation of allylsilane and vinylsilane shown in Figure 3.

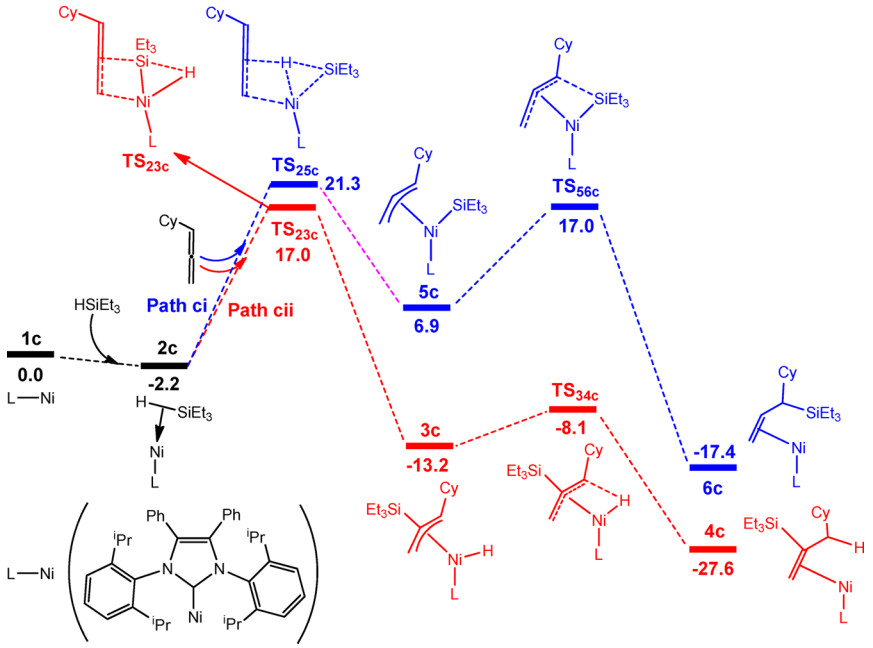

Figure 5. Free-energy profiles calculated for the allene hydrosilylation catalyzed by bulky N-heterocyclic carbene complex of nickel for the formation of allylsilane (path **ci**) and vinylsilane (path **cii**). The relative free energies in the solvent are given in kcal/mol.

dx.doi.org/10.1021/jo500557w | J. Org. Chem. 2014, 79, 4517−4527

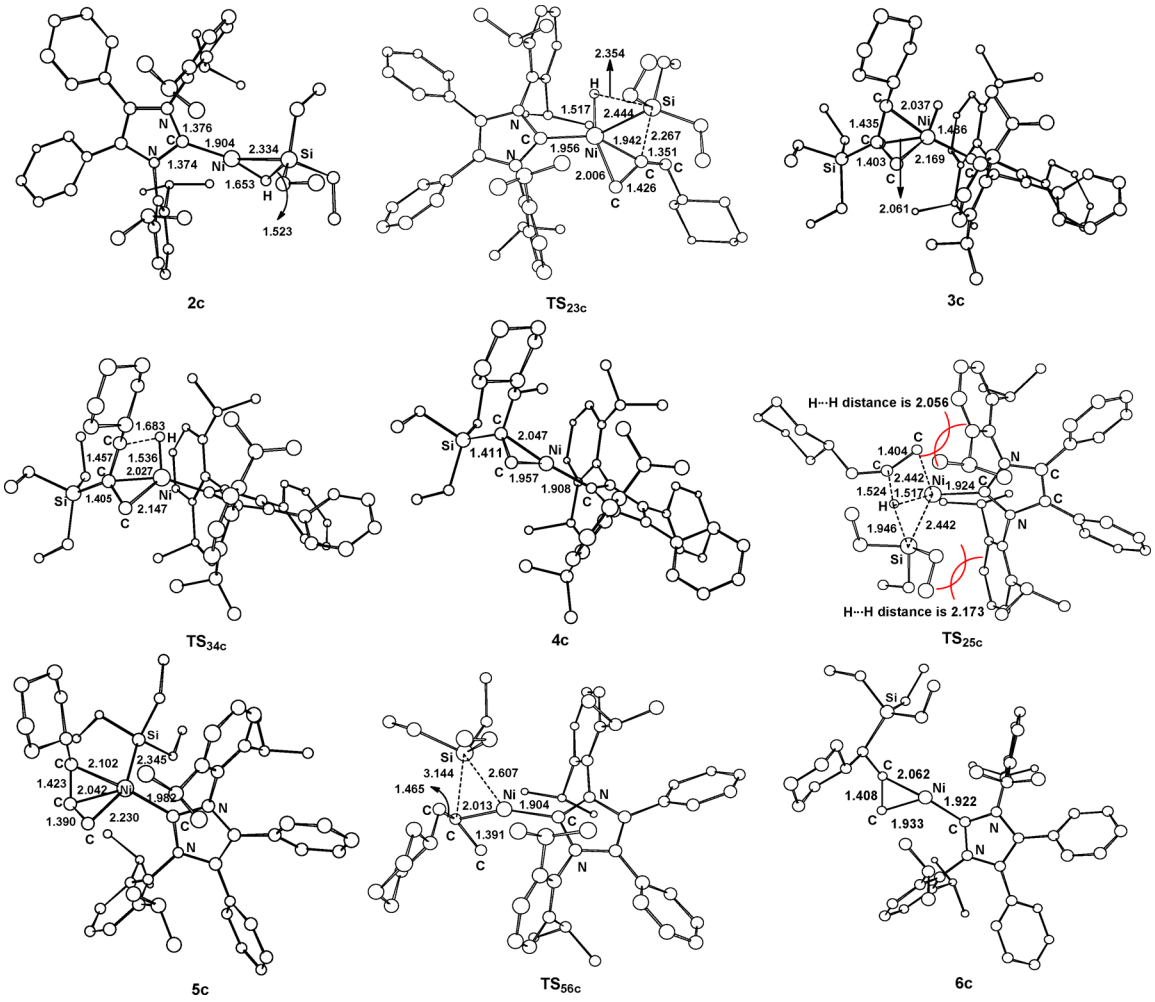

Figure 6. Optimized species involved in the allene hydrosilylation catalyzed by bulky N-heterocyclic carbene complex of nickel for the formation of vinylsilane and allylsilane shown in Figure 5.

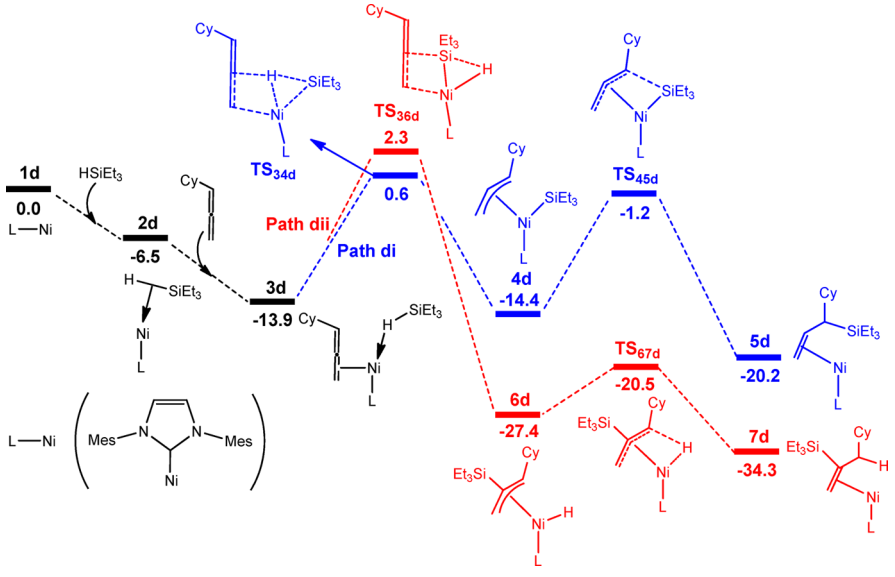

Figure 7. Free-energy profiles calculated for the allene hydrosilylation catalyzed by a small N-heterocyclic carbene complex of nickel for the formation of allylsilane (path **di**) and vinylsilane (path **dii**). The relative free energies in the solvent are given in kcal/mol.

We then consider the allene hydrosilylation catalyzed by the small N-heterocyclic carbene complex of nickel. Figure 7 shows the free-energy profiles for the formation of allylsilane (path **di**) and vinylsilane (path **dii**). The corresponding optimized structures

dx.doi.org/10.1021/jo500557w | J. Org. Chem. 2014, 79, 4517−4527

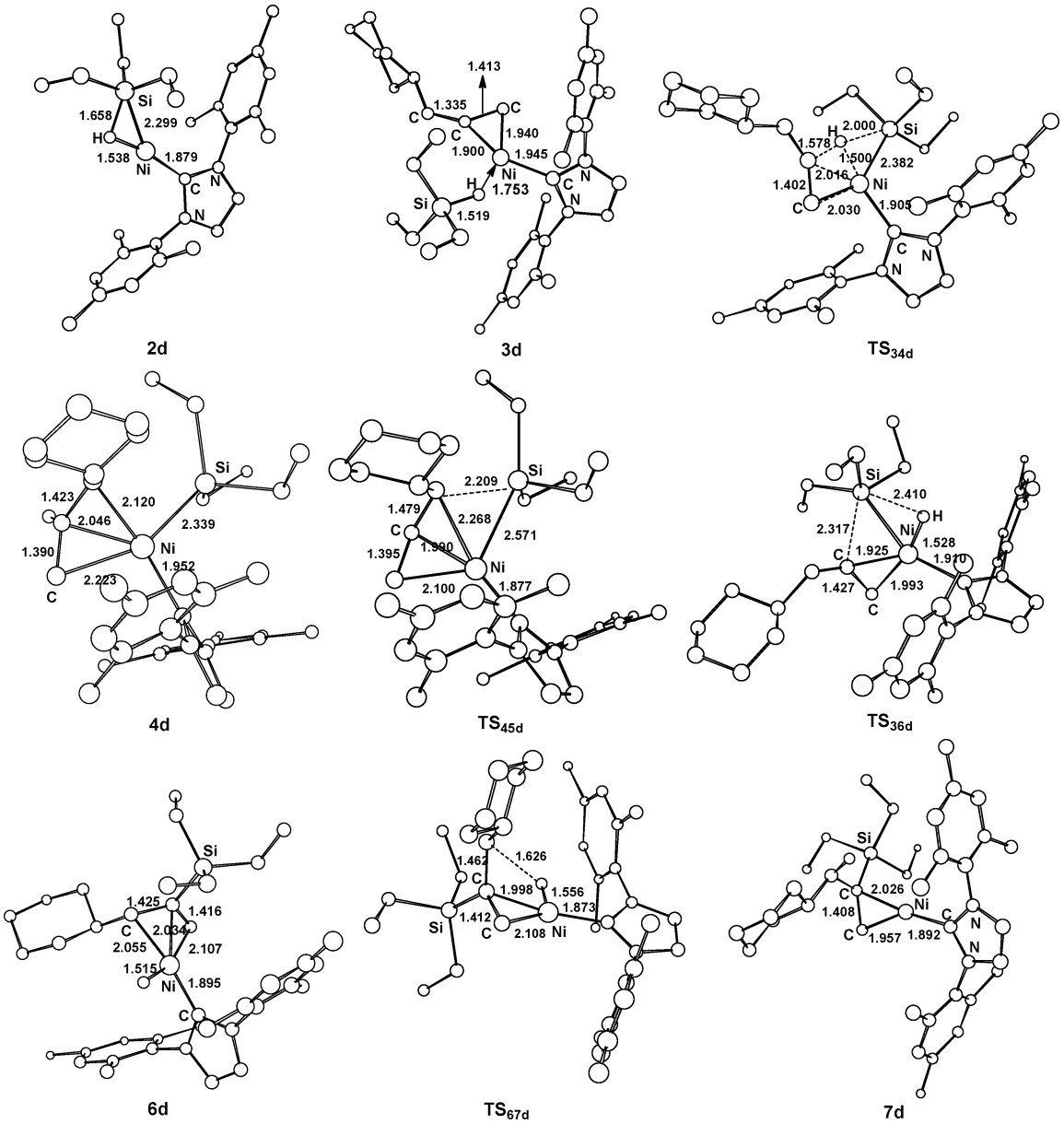

Figure 8. Optimized species involved in the allene hydrosilylation catalyzed by a small N-heterocyclic carbene complex of nickel for the formation of allylsilane and vinylsilane shown in Figure 7.

with selected structural parameters are presented in Figure 8. The calculation results show that the catalytic mechanism is similar to that of Pd-catalyzed allene hydrosilylation with a small NHC ligand shown in Figure 1. Path **di** considers the reaction for the formation of allylsilane, and the Si−H bond oxidative addition concerted with hydride insertion is the rate-determining step needing a barrier ($\mathbf{TS}_{34d}$) of 14.5 kcal/mol. Path **dii** involves the reaction for the formation of vinylsilane, and the Si−H bond oxidative addition concerted with silyl insertion is the rate-limiting step requiring a barrier ($\mathbf{TS}_{36d}$) of 16.2 kcal/mol. The calculations indicate that the barrier for path **di** is lower than path **dii** by 1.7 kcal/mol, which is in accord with the experimental observations that the allylsilane is the major product for small Ni catalyst (allylsilane/vinylsilane = 67:33).[17]

Comparison of Palladium and Nickel Catalysts with Small and Bulky NHC Ligands for Regioselective Allene Hydrosilylation. On the basis of the calculations for the use of palladium catalyst with small NHC ligand, path **ai** involving the formation of the allylsilane is kinetically more favorable than path **aii** involving the formation of the vinylsilane (Figure 1). While utilizing bulky NHC ligand with palladium, the barriers for both reactions are obviously high with the values of 41.6 kcal/mol (path **bi** in Figure 3) and 40.2 kcal/mol (path **bii**) due to the strong steric repulsions between the bulky NHC ligand with the silyl group and allene, indicating that both reactions are kinetically unfavorable, which can be confirmed by experimental observations that the product yields of allylsilane and vinylsilane are trace and the regioselectivity is not determined.[17] For the use of nickel catalyst with bulky NHC ligand, path **cii** involving the formation of the vinlylsilane is both kinetically and thermodynamically more favored than path **ci** involving the formation of the allylsilane (Figure 5). While using small NHC ligand with nickel, path **di** involving the formation of the allylsilane is kinetically more favorable than path **dii** involving the formation of the vinylsilane (Figure 7).

dx.doi.org/10.1021/jo500557w | J. Org. Chem. 2014, 79, 4517−4527

All calculation results are consistent with observed regioselectivities.[17]

For the region control, the important step in the catalytic cycle is oxidative addition of the Si−H bond concerted with hydride or silyl insertion, for which a rationalization is proposed below. Both electronic and steric factors play a key role in the reactivities and regioselectivities for the hydrosilylation of allene via Pd and Ni catalysts. For the hydrosilylation of allene via Pd catalyst with small NHC ligand, electronically, the allene central carbon is electrophilic, which facilitates the rate-limiting hydride insertion, leading to the formation of allylsilane as the major product. Sterically, the interactions provided by the NHC moiety with the silyl group and allene are small. The electronic influences could be reversed via the steric effect offered by bulky NHC ligand. For the hydrosilylation of allene via Pd catalyst with bulky NHC ligand, the steric interactions provided by the NHC moiety with the silyl group and allene are significantly large, and both reactions for the formation of allylsilane and vinylsilane are kinetically unfavorable. On the other hand, for the hydrosilylation of allene by Ni catalyst with bulky NHC ligand, the steric effect is matched with electronic effect to obtain high regiocontrol. In contrast to small NHC ligand, the regioselectivity for bulky NHC ligand of Ni catalyst is enhanced and the electronic nature of the Ni center and bulky NHC ligand favor the silyl insertion, leading to the formation of vinylsilane.

We also consider the different catalytic activity of Pd and Ni catalysts with bulky and small NHC ligands. For the Pd catalyst with bulky NHC ligand (Figure 3), the Si−H bond oxidative addition concerted with hydride insertion is the rate-limiting step in path **bi** requiring a barrier ($\mathbf{TS}_{23b}$) of 41.6 kcal/mol, and the Si−H bond oxidative addition concerted with silyl insertion is the rate-limiting step in path **bii** needing a barrier ($\mathbf{TS}_{25b}$) of 40.2 kcal/mol. For the Ni catalyst with bulky NHC ligand (Figure 5), the Si−H bond oxidative addition concerted with silyl insertion is the rate-limiting step with a barrier ($\mathbf{TS}_{23c}$) of 19.2 kcal/mol, and the Si−H bond oxidative addition concerted with hydride insertion is the rate-limiting step requiring a barrier ($\mathbf{TS}_{25c}$) of 23.5 kcal/mol. On the basis of the calculations, the Pd and Ni catalysts with bulky NHC ligand show the different catalytic activity. We first checked the geometry differences between $\mathbf{TS}_{23b}$ and $\mathbf{TS}_{23c}$, $\mathbf{TS}_{25b}$ and $\mathbf{TS}_{25c}$, and it exhibits no obvious difference. We then considered the electronic effects between $\mathbf{TS}_{23b}$ and $\mathbf{TS}_{23c}$, $\mathbf{TS}_{25b}$ and $\mathbf{TS}_{25c}$. The NBO charges of Pd and Ni complexes are shown in Scheme 5. We know that Ni and Pd belong to group 10 metals, and Ni is more apt to lose two electrons than Pd. As shown in Figures 3 and 5, four transition states are involved in the oxidative addition step; thus, $\mathbf{TS}_{23c}$ and $\mathbf{TS}_{25c}$ involving the Ni catalyst have relatively low barriers compared to $\mathbf{TS}_{23b}$ and $\mathbf{TS}_{25b}$ involving the Pd catalyst. The same trends could also be found in Figures 1 and 7 involving the Pd and Ni catalysts with small NHC ligands.

Scheme 5. NBO Charges of the Pd and Ni Complexes

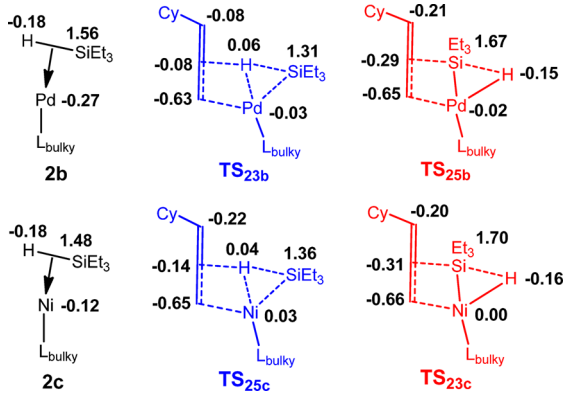

CONCLUSIONS

In this work, we have theoretically investigated the hydrosilylation of allene via Pd and Ni catalysts with small and bulky NHC ligands to clarify the reaction mechanisms and origins of the regioselectivities for the formation of allylsilane and vinylsilane. The reaction mechanism is found to contain three steps for the hydrosilylation of allene via Pd and Ni catalysts: (1) coordination of $HSiEt_3$ and allene to the Pd or Ni center; (2) subsequent Si−H bond oxidative addition concerted with hydride or silyl insertion; (3) reductive elimination to afford the product and regenerates the catalyst. The calculations show that the concerted step is the rate-limiting step for the whole catalytic cycle.

The regioselectivity is involved in the concerted step, and the calculations demonstrate that the regioselectivity is predominantly governed by the metals and ligands. Different metals (Ni vs Pd) can lead to regiochemical reversals for the hydrosilylation of allene. Allylsilane is the major product via palladium catalysis with small NHC ligand, while vinylsilane is the major product via nickel catalysis with bulky NHC ligand. Moreover, changing the structure of NHC ligand further improves the regioselectivities to generate vinylsilane or allylsilane in high yields with exceptional regiocontrol. The regioselectivity for vinylsilane product using nickel is enhanced with bulky NHC ligand, whereas regioselectivity for allylsilane using palladium is enhanced with small NHC ligand.

The results show that high selectivity is attainable by appropriate choice of the metals and the ligands of the catalysts in the hydrosilylation reactions. We expect that our calculations are helpful for the theoretical design of new catalysts for the regioselectivity of hydrosilylation reactions.

ASSOCIATED CONTENT

Supporting Information

Cartesian coordinates of all species. This material is available free of charge via the Internet at http://pubs.acs.org.

AUTHOR INFORMATION

Corresponding Authors

*E-mail: hujunxie@gmail.com. Fax: +86-571-28008900.
*E-mail: xiongch@163.com. Fax: +86-571-28008900.

Notes

The authors declare no competing financial interest.

ACKNOWLEDGMENTS

This work was supported by the National Science Foundation of China (21203166, 91127010, and 21273201) and the Natural Science Foundation of Zhejiang Province (Y4100620 and LY12B04003). We also thank the anonymous reviewers for their constructive suggestions and comments.

REFERENCES

(1) (a) Fleming, I.; Barbero, A.; Walter, D. *Chem. Rev.* **1997**, *97*, 2063. (b) Ojima, I. In *The Chemistry of Organic Silicon Compounds*;

Patai, S., Rappoport, Z., Eds.; Wiley: Chichester, UK, 1989; Vol. *1*, Chapter 25. (c) Hiyama, T.; Kusumoto, T. In *Comprehensive Organic Synthesis*; Trost, B. M., Fleming, I., Eds.; Pergamon Press: Oxford, 1991; Vol. *8*, Chapter 3.12. (d) *Comprehensive Handbook on Hydrosilylation*; Marciniec, B., Ed.; Pergamon Press: Oxford, 1992. (e) Marciniec, B.; Maciejewski, H.; Pietraszuk, C.; Pawluc, P. In *Hydrosilylation: A Comprehensive Review on Recent Advances*; Marciniec, B., Ed.; Advances in Silicon Science; Springer: Berlin, 2009; Vol. *1*, Chapters 2 and 3.

(2) (a) Nakao, Y.; Hiyama, T. *Chem. Soc. Rev.* **2011**, *40*, 4893. (b) Chang, W. T. T.; Smith, R. C.; Regens, C. S.; Bailey, A. D.; Werner, N. S.; Denmark, S. E. *Org. React.* **2011**, *75*, 213.

(3) (a) Hosomi, A.; Endo, M.; Sakurai, H. *Chem. Lett.* **1976**, 941. (b) Masse, C. E.; Panek, J. S. *Chem. Rev.* **1995**, *95*, 1293.

(4) (a) Lewis, L. N.; Stein, J.; Gao, Y.; Colborn, R. E.; Hutchins, G. *Platinum Metals Rev.* **1997**, *41*, 66. (b) Stein, J.; Lewis, L. N.; Gao, Y.; Scott, R. A. *J. Am. Chem. Soc.* **1999**, *121*, 3693. (c) Marciniec, B.; Maciejewski, H.; Pietraszuk, C.; Pawluc, P. In *Advances in Silicon Science*, 1st ed.; Matisons, J., Ed.; Springer: New York, 2009; Vol. *1*. (d) Clarson, S. J. *Silicon* **2009**, *1*, 57.

(5) (a) Glaser, P. B.; Tilley, T. D. *J. Am. Chem. Soc.* **2003**, *125*, 13640. (b) Beddie, C.; Hall, M. B. *J. Am. Chem. Soc.* **2004**, *126*, 13564. (c) Brunner, H. *Angew. Chem., Int. Ed.* **2004**, *43*, 2749.

(6) Sommer, L. H.; Pietrusza, E. W.; Whitmore, F. C. *J. Am. Chem. Soc.* **1947**, *69*, 188.

(7) Wagner, G. H. Union Carbide and Carbon Corp., US2637738 A, 1953.

(8) Adamski, A.; Kubicki, M.; Pawluc, P.; Grabarkiewicz, T.; Patroniak, V. *Catal. Commun.* **2013**, *42*, 79.

(9) Sumida, Y.; Kato, T.; Yoshida, S.; Hosoya, T. *Org. Lett.* **2012**, *14*, 1552.

(10) Zhou, H.; Moberg, C. *Org. Lett.* **2013**, *15*, 1444.

(11) Liu, L.; Li, X. N.; Dong, H.; Wu, C. *J. Organomet. Chem.* **2013**, *745*−*746*, 275.

(12) De Bo, G.; Berthon-Gelloz, G.; Tinant, B.; Marko, I. E. *Organometallics* **2006**, *25*, 1881. (b) Troegel, D.; Stohrer, J. *Coord. Chem. Rev.* **2011**, *255*, 1440. (c) Marko, I. E.; Sterin, S.; Buisine, O.; Mignani, G.; Branlard, P.; Tinant, B.; Declercq, J. P. *Science* **2002**, *298*, 204.

(13) (a) Kawasaki, Y.; Ishikawa, Y.; Igawa, K.; Tomooka, K. *J. Am. Chem. Soc.* **2011**, *133*, 20712. (b) Rankin, M. A.; MacLean, D. F.; Schatte, G.; McDonald, R.; Stradiotto, M. *J. Am. Chem. Soc.* **2007**, *129*, 15855. (c) Berthon-Gelloz, G.; Marko, I. E. In *N-Heterocyclic Carbenes in Synthesis*, 1st ed.; Nolan, S. P., Ed.; Wiley-VCH: Weinheim, 2006; pp 119−162. (d) Belger, C.; Plietker, B. *Chem. Commun.* **2012**, *48*, 5419. (e) Rooke, D. A.; Ferreira, E. M. *Angew. Chem., Int. Ed.* **2012**, *51*, 3225. (f) Berthon-Gelloz, G.; Schumers, J. M.; De Bo, G.; Marko, I. E. *J. Org. Chem.* **2008**, *73*, 4190. (g) Zeng, J. Y.; Hsieh, M. H.; Lee, H. M. *J. Organomet. Chem.* **2005**, *690*, 5662.

(14) (a) Trost, B. M.; Ball, Z. T. *J. Am. Chem. Soc.* **2001**, *123*, 12726. (b) Trost, B. M.; Ball, Z. T. *J. Am. Chem. Soc.* **2005**, *127*, 17644.

(15) Wu, J. Y.; Stanzl, B. N.; Ritter, T. *J. Am. Chem. Soc.* **2010**, *132*, 13214.

(16) Sudo, T.; Asao, N.; Gevorgyan, V.; Yamamoto, Y. *J. Org. Chem.* **1999**, *64*, 2494.

(17) Miller, Z. D.; Li, W.; Belderrain, T. R.; Montgomery, J. *J. Am. Chem. Soc.* **2013**, *135*, 15282.

(18) (a) Becke, A. D. *J. Chem. Phys.* **1993**, *98*, 5648. (b) Lee, C.; Yang, W.; Parr, R. G. *Phys. Rev. B* **1988**, *37*, 785. (c) Becke, A. D. *J. Chem. Phys.* **1993**, *98*, 1372. (d) Becke, A. D. *Phys. Rev. B* **1988**, *38*, 3098.

(19) (a) Xie, H. J.; Zhang, H.; Lin, Z. Y. *Organometallics* **2013**, *32*, 2336. (b) Xie, H. J.; Lin, F. R.; Lei, Q. F.; Fang, W. J. *Organometallics* **2013**, *32*, 6957. (c) Xie, H. J.; Zhang, H.; Lin, Z. Y. *New J. Chem.* **2013**, *37*, 2856. (d) Xie, H. J.; Lin, F. R.; Yang, L.; Chen, X. S.; Ye, X. C.; Tian, X.; Lei, Q. F.; Fang, W. J. *J. Organomet. Chem.* **2013**, *745*−*746*, 417. (e) Xie, H. J.; Lin, F. R.; Lei, Q. F.; Fang, W. J. *J. Phys. Org. Chem.* **2013**, *26*, 933. (f) Yang, L.; Ren, G. R.; Ye, X. C.; Que, X. Y.; Lei, Q. F.; Fang, W. J.; Xie, H. J. *J. Phys. Org. Chem.* **2014**, *27*, 237.

(20) (a) Tang, S. Y.; Guo, Q. X.; Fu, Y. *Chem.—Eur. J.* **2011**, *49*, 13866. (b) Perez-Rodriguez, M.; Braga, A. A. C.; de Lera, A. R.; Maseras, F.; Alvarez, R.; Espinet, P. *Organometallics* **2010**, *29*, 4983. (c) Surawatanawong, P.; Hall, M. B. *Organometallics* **2008**, *27*, 6222. (d) Lam, K. C.; Marder, T. B.; Lin, Z. Y. *Organometallics* **2010**, *29*, 1849. (e) Xue, L. Q.; Lin, Z. Y. *Chem. Soc. Rev.* **2010**, *39*, 1692. (f) Yu, H. Z.; Fu, Y.; Guo, Q. X.; Lin, Z. Y. *Organometallics* **2009**, *28*, 4507. (g) Zheng, W. X.; Ariafard, A.; Lin, Z. Y. *Organometallics* **2008**, *27*, 246. (h) Lam, K. C.; Marder, T. B.; Lin, Z. Y. *Organometallics* **2007**, *26*, 758. (i) Ariafard, A.; Lin, Z. Y. *J. Am. Chem. Soc.* **2006**, *128*, 13010.

(21) (a) Check, C. E.; Faust, T. O.; Bailey, J. M.; Wright, B. J.; Gilbert, T. M.; Sunderlin, L. S. *J. Phys. Chem. A* **2001**, *105*, 8111. (b) Hay, P. J.; Wadt, W. R. *J. Chem. Phys.* **1985**, *82*, 299.

(22) Ehlers, A. W.; Bohme, M.; Dapprich, S.; Gobbi, A.; Hollwarth, A.; Jonas, V.; Kohler, K. F.; Stegmann, R.; Veldkamp, A.; Frenking, G. *Chem. Phys. Lett.* **1993**, *208*, 111.

(23) Huzinaga, S. *Gaussian Basis Sets for Molecular Calculations*; Elsevier Science: Amsterdam, 1984.

(24) (a) Fukui, K. *J. Phys. Chem.* **1970**, *74*, 4161. (b) Fukui, K. *Acc. Chem. Res.* **1981**, *14*, 363.

(25) Gaussian 09, Revision A.1: Frisch, M. J.; Trucks, G.. W.; Schlegel, H. B.; Scuseria, G. E.; Robb, M. A.; Cheeseman, J. R.; Scalmani, G.; Barone, V.; Mennucci, B.; Petersson, G. A.; Nakatsuji, H.; Caricato, M.; Li, X.; Hratchian, H. P.; Izmaylov, A. F.; Bloino, J.; Zheng, G.; Sonnenberg, J. L.; Hada, M.; Ehara, M.; Toyota, K.; Fukuda, R.; Hasegawa, J.; Ishida, M.; Nakajima, T.; Honda, Y.; Kitao, O.; Nakai, H.; Vreven, T.; Montgomery, J. A., Jr.; Peralta J. E.; Ogliaro, F.; Bearpark, M.; Heyd, J. J.; Brothers, E.; Kudin, K. N.; Staroverov, V. N.; Kobayashi, R.; Normand, J.; Raghavachari, K.; Rendell, A.; Burant, J. C.; Iyengar, S. S.; Tomasi, J.; Cossi, M.; Rega, N.; Millam, J. M.; Klene, M.; Knox, J. E.; Cross, J. B.; Bakken, V.; Adamo, C.; Jaramillo, J.; Gomperts, R.; Stratmann, R. E.; Yazyev, O.; Austin, A. J.; Cammi, R.; Pomelli, C.; Ochterski, J. W.; Martin, R. L.; Morokuma, K.; Zakrzewski, V. G.; Voth, G. A.; Salvador, P.; Dannenberg, J. J.; Dapprich, S.; Daniels, A. D.; Farkas, O.; Foresman, J. B.; Ortiz, J. V.; Cioslowski, J.; Fox, D. J. Gaussian, Inc., Wallingford, CT, 2009.

(26) Barone, V.; Cossi, M. *J. Phys. Chem. A* **1998**, *102*, 1995. (b) Cossi, M.; Rega, N.; Scalmani, G.; Barone, V. *J. Comput. Chem.* **2003**, *24*, 669.

(27) Benson, S. W. *The Foundations of Chemical Kinetics*; Krieger: Malabar, FL, 1982.

(28) (a) Okuno, Y. *Chem.—Eur. J.* **1997**, *3*, 212. (b) Ardura, D.; López, R.; Sordo, T. L. *J. Phys. Chem. B* **2005**, *109*, 23618. (c) Schoenebeck, F.; Houk, K. N. *J. Am. Chem. Soc.* **2010**, *132*, 2496. (d) Liu, Q.; Lan, Y.; Liu, J.; Li, G.; Wu, Y. D.; Lei, A. *J. Am. Chem. Soc.* **2009**, *131*, 10201. (e) Wang, M. Y.; Fan, T.; Lin, Z. Y. *Organometallics* **2012**, *31*, 560. (f) Wang, M. Y.; Fan, T.; Lin, Z. Y. *Polyhedron* **2012**, *32*, 35. (g) Liu, B. W.; Gao, M.; Dang, L.; Zhao, H. T.; Marder, T. B.; Lin, Z. Y. *Organometallics* **2012**, *31*, 3410.

(29) (a) Choi, S. H.; Feng, J. W.; Lin, Z. Y. *Organometallics* **2000**, *19*, 2051. (b) Corey, J. Y.; Braddock-Wilking. *J. Chem. Rev.* **1999**, *99*, 175. (c) Speier, J. L. *Adv. Organomet. Chem.* **1977**, *17*, 407. (d) Parshall, G. W. *Homogeneous Catalysis: the Application and Chemistry of Catalysis by Soluble Transition Metal Complexes*; Wiley: New York, 1992; p 39.

(30) Pyykkö, P.; Atsumi, M. *Chem.—Eur. J.* **2009**, *15*, 12770.

(31) Popp, B. V.; Stahl, S. S. *J. Am. Chem. Soc.* **2007**, *129*, 4410.

(32) Iglesias, M.; Sanz Miguel, P. J.; Polo, V.; Fernandez-Alvarez, F. J.; Perez-Torrente, J. J.; Oro, L. A. *Chem.—Eur. J.* **2013**, *19*, 17559.

(33) Chung, L. W.; Wu, Y. D.; Trost, B. M.; Ball, Z. T. *J. Am. Chem. Soc.* **2003**, *125*, 11578. (b) Lam, W. H.; Lin, Z. *Organometallics* **2003**, *22*, 473. (c) Lam, W. H.; Jia, G.; Lin, Z.; Lau, C. P.; Eisenstein, O. *Chem.—Eur. J.* **2003**, *9*, 2775.

(34) (a) Abe, Y.; Kuramoto, K.; Ehara, M.; Nakatsuji, H.; Suginome, M.; Murakami, M.; Ito, Y. *Organometallics* **2008**, *27*, 1736. (b) Suginome, M.; Ohmori, Y.; Ito, Y. *J. Organomet. Chem.* **2000**, *611*, 403.

(35) (a) Obora, Y.; Tsuji, Y.; Kawamura, T. *J. Am. Chem. Soc.* **1993**, *115*, 10414. (b) Obora, Y.; Tsuji, Y.; Kawamura, T. *J. Am. Chem. Soc.* **1995**, *117*, 9814. (c) Tsuji, Y.; Funato, M.; Ozawa, M.; Ogiyama, H.;

Kajita, S.; Kawamura, T. *J. Org. Chem.* **1996**, *61*, 5779. (d) Sakaki, S.; Satoh, H.; Shomo, H.; Ujino, Y. *Organometallics* **1996**, *15*, 1713. (e) Biswas, B.; Sugimoto, M.; Sakaki, S. *Organometallics* **1999**, *18*, 4015.

(36) (a) Reed, A. E.; Weinstock, R. B.; Weinhold, F. *J. Chem. Phys.* **1985**, *83*, 735. (b) Reed, A. E.; Weinhold, F. *J. Chem. Phys.* **1985**, *83*, 1736. (c) Reed, A. E.; Curtiss, L. A.; Weinhold, F. *Chem. Rev.* **1988**, *88*, 899.

(37) (a) Bai, T.; Zhu, J.; Xue, P.; Sung, H. H. Y.; Williams, I. D.; Ma, S. M.; Lin, Z. Y.; Jia, G. C. *Organometallics* **2007**, *26*, 5581. (b) Bai, T.; Xue, L. Q.; Xue, P.; Zhu, J.; Sung, H. H. Y.; Ma, S. M.; Wiliams, I. D.; Lin, Z. Y.; Jia, G. C. *Organometallics* **2008**, *27*, 2614.

(38) (a) Brookhart, M.; Volpe, A. F.; Lincoln, D. M.; Horvath, I. T.; Limmar, J. M. *J. Am. Chem. Soc.* **1990**, *112*, 5634. (b) Brookhart, M.; Hauptman, E.; Lincoln, D. M. *J. Am. Chem. Soc.* **1992**, *114*, 10394.